Turkish Journal of Electrical Engineering & Computer Sciences

http://journals.tubitak.gov.tr/elektrik/

Research Article

Turk J Elec Eng & Comp Sci
(2016) 24: 5238 – 5250

doi:10.3906/elk-1412-6

Dynamic characteristics of an isolated self-excited synchronous reluctance generator driven by a wind turbine

Mosaad Mohiedden ALI[1,*], **Said Mahmoud ALLAM**[2], **Talaat Hamdan ABDEL-MONEIM**[3]
[1]Department of Electrical Engineering, Kafrelshiekh University, Kafrelshiekh, Egypt
[2]Department of Electrical Power and Machines Engineering, Tanta University, Tanta, Egypt
[3]Department of Electrical Engineering, Alexandria University, Alexandria, Egypt

Received: 08.12.2014 • **Accepted/Published Online:** 07.11.2015 • **Final Version:** 06.12.2016

Abstract: This paper studies the dynamic characteristics of an isolated three-phase self-excited synchronous reluctance generator (SESRG) driven by a variable-speed wind turbine under different operating conditions. Self-excitation is achieved via capacitors connected across the generator terminals. A detailed mathematical modeling of the proposed self-excited wind generation system is presented. The proposed analysis is based on the dynamic qd-axis model of the SESRG. Magnetic saturation is taken into account and is assumed to be confined to the direct axis and is accounted for as a variable direct-axis magnetizing reactance. Effect of wind-speed variation, excitation-capacitance variation, and loading-conditions variation on the generated output voltage and frequency are presented and discussed. The presented results show the effectiveness of the proposed wind-generation system. A close agreement between experimental and simulated results has been observed, which supports the validity of the proposed analysis.

Key words: Dynamic characteristics, isolated, self-excited, synchronous reluctance generator, wind energy

1. Introduction

Over the last 20 years, renewable energy sources have been attracting great attention due to increasing prices and reduction of conventional energy sources. In addition, the air pollution of fossil fuel affects both the environment and human health [1]. Solar energy, wind energy, geothermal heat, hydroelectricity, biofuels, biomass, and nuclear energy represent the most important types of renewable energy sources to date. Wind energy is one of the fastest growing renewable energy sources compared to other sources of renewable energy. Thousands of wind turbines are being invested and installed everywhere worldwide [2]. Therefore, the need for alternative and renewable energy sources for utility and autonomous applications, especially in remote areas, has focused attention on the use of electric generators driven by wind turbines.

In particular, brushless self-excited generators such as squirrel-cage induction generators and synchronous reluctance generators are found to be of great potential as very attractive supply options for industrial and domestic applications. Preference is given to such generator types because of their simpler construction, robustness, absence of current collection brushes, low cost, and maintenance-free operation [3–5]. Hence, such generators represent ideal candidates as wind-generating conversion systems, especially for low- and medium-power applications [6–8]. Moreover, they have the ability to convert mechanical power to electrical power over a wide range of wind speeds.

*Correspondence: epe_mosaad@eng.kfs.edu.eg

Self-excitation of such generators is achieved via capacitors connected to the machine terminals. Such self-excitation overcomes the need for an external power supply to produce the excitation magnetic field. In addition to being simple, robust, and inexpensive as induction generators, self-excited synchronous reluctance generators (SESRGs) have low core loss, low noise, and low rotor copper loss and they reveal a well-defined relationship between rotor speed and output frequency [9]. Furthermore, SESRGs have no cogging torque. Hence, wind-generation systems with such generators can achieve a smooth starting behavior at low wind velocity [6]. This motivated the researchers to analyze the performance characteristics of a SESRG especially when driven by a wind turbine.

Some studies discussed the performance characteristics and steady-state analysis of synchronous reluctance generators [10–12]. In addition, a little work has been presented on the transient analysis of this generator type [13–15]. On the other hand, the performance analysis of SESRGs when driven by a wind turbine has not gained significant attention from researchers to date [6,16]. In fact, performance characteristics of SESRGs in wind generating should be studied under different operating conditions.

Therefore, this paper concentrates on the dynamic analysis of a wind-driven SESRG under different operating conditions. It also describes how the operating frequency and generated voltage are affected by any variation in load condition, machine parameters, excitation capacitor rating, and rotor speed. Experimental results are compared with simulation results in order to support the validity of the proposed study.

2. Proposed self-excited wind generating system

Figure 1 shows the schematic diagram of the proposed self-excited wind generating system configuration. The proposed system consists of the following:

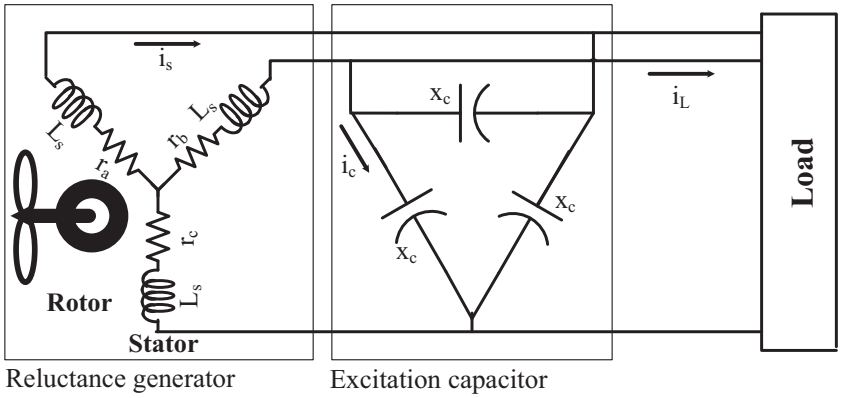

Figure 1. Schematic diagram of the proposed self-excited wind generating system.

- Wind turbine
- Synchronous reluctance generator
- Balanced three-phase excitation capacitors
- Balanced three-phase load

The excitation capacitors are used to ensure the self-excitation process. First, at a suitable value of the prime mover speed and aided with the machine residual magnetism, a small stator voltage will be induced.

This induced voltage causes an excitation current to flow through the excitation capacitors. This results in an additional increase in the stator induced voltage. The increase in both excitation current and induced stator voltage continues until steady-state condition occurs due to inherent machine magnetic saturation [10,17].

The machine magnetizing characteristics consider the main factor for voltage build-up behavior and stabilization of generated voltage of the self-excited generators. At certain loading conditions and prime-mover speed with an appropriate value of excitation-capacitance, the voltage continues to build up until it reaches a steady state [7,18]. On the other hand, it is well known that in the case of reluctance generators the frequency of generated voltage depends only upon the mechanical speed and is thus easier to control [14]. In the following sections the overall system modeling is presented, including both the wind-turbine model and the synchronous reluctance generator model. Hence, the effect of different operating conditions on the system performance characteristics is investigated both theoretically and experimentally.

3. System modeling

3.1. Wind-turbine model

It is well known that the energy contained by the wind is in the form of kinetic energy. This energy converts into mechanical energy aided by the wind turbine. The wind-turbine model is normally described by a set of characteristic equations, from which the performance characteristics of the wind turbine can be easily obtained. These equations can be summarized as follows.

The overall wind power is proportional to cubic wind speed and the rotor-swept area [2,19]. This power can be written as:

$$P_w = \frac{1}{2}\,\rho A V_w^3 \tag{1}$$

A fraction of the overall wind power is converted into mechanical power. The mechanical power captured by the wind turbine can be expressed as:

$$P_m = P_w \times C_p. \tag{2}$$

The rotor-power coefficient C_p is a very important design factor that gives the fraction of the kinetic energy (overall wind power) that is converted into mechanical energy.

The characteristic of the rotor-power coefficient depends mainly on the turbine tip-speed ratio, λ, and the blade pitch-angle, β. The rotor-power coefficient can be expressed as a function of tip-speed ratio and blade pitch-angle (λ, β) using the following empirical formulas [20].

$$C_p(\lambda,\beta) = c1 \times \left\{ \frac{c2}{\lambda_i} - c3 \times \beta - c4 \right\} \times e^{-\frac{c5}{\lambda_i}} + c6 \times \lambda \tag{3}$$

$$\frac{1}{\lambda_i} = \left(\frac{1}{\lambda + 0.08\beta} - \frac{0.035}{1+\beta^3} \right) \tag{4}$$

Where, values of the constants are [20]: c1 = 0.5176, c2 = 116, c3 = 0.4, c4 = 5, c5 = 21, c6 = 0.0068.

The tip-speed ratio is defined as the ratio of the turbine-blade linear speed and the actual wind speed. The tip-speed ratio is given by [19]:

$$\lambda = \frac{R\omega_r}{V_w}. \tag{5}$$

Figure 2 shows the relationship between the rotor-power coefficient and the tip-speed ratio at a blade pitch-angle of 7°. It can be observed that, at a certain value of blade pitch-angle, there is only one value of the tip-speed ratio at which the power coefficient is maximum [2].

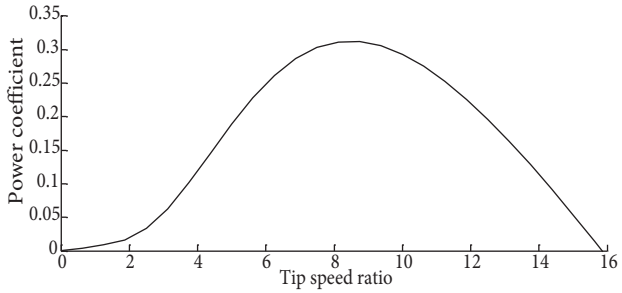

Figure 2. Characteristics of rotor power coefficient over tip-speed ratio at pitch angle of 7°.

The mechanical output power can be rewritten in terms of wind-turbine characteristics as:

$$P_m = \frac{\rho \pi R^2 C_p(\beta, \lambda) V_w^3}{2}. \tag{6}$$

Finally, the output torque of the wind-turbine, which considers the input torque of the SESRG, can be calculated as:

$$T_m = \frac{P_w}{\omega_r} = \frac{\rho \pi R^3 C_p(\beta, \lambda) V_w^2}{2\lambda}. \tag{7}$$

3.2. Synchronous reluctance generator model

A simplified mathematical model of the SESRG is introduced on the basis of Park's qd-axis model. The saturation effect on the direct axis magnetizing inductance is always considered as it is a requisite to provide a stable operating condition.

In order to simplify the analysis of the self-excited reluctance generator, the following assumptions are taken into consideration [9,11,12]:

- The saturation effect on the machine parameters other than the d-axis magnetizing inductance reactance is ignored.
- The core losses are neglected.

In addition, the proposed SESRG model has been developed considering the existence of a squirrel cage associated with the synchronous reluctance rotor. Therefore, the rotor is represented as two damper-windings in both the direct axis and quadrature axis directions. The stator and rotor voltage equations are represented in the qd-axis rotor reference frame in order to eliminate the time-varying inductances [14,21]. The final qd-axis model of the proposed SESRG can be written as follows.

The qd-axis voltage equations can be written as shown below.

$$V_{qs} = p\,\lambda_{qs} + \omega_r\,\lambda_{ds} - r_a i_q \tag{8}$$

$$V_{ds} = p\,\lambda_{ds} - \omega_r\,\lambda_{qs} - r_a i_d \tag{9}$$

$$V_{dr} = p\,\lambda_{dr} + r_{dr} i_{dr} \tag{10}$$

$$V_{qr} = p\,\lambda_{qr} + r_{qr} i_{qr} \tag{11}$$

The stator and rotor winding flux linkages can be expressed in terms of machine currents and inductances as follows.

$$\lambda_{ds} = -L_{ds} i_{ds} + L_{md} i_{dr} \tag{12}$$

$$\lambda_{qs} = -L_{qs} i_{qs} + L_{mq} i_{qr} \tag{13}$$

$$\lambda_{qr} = -L_{mq} i_{qs} + L_{qr} i_{qr} \tag{14}$$

$$\lambda_{dr} = -L_{md} i_{ds} + L_{dr} i_{dr} \tag{15}$$

If the generator is loaded with a pure resistive load, the resultant qd-axis load current equations can be written as follows. [13]

$$i_{lq} = v_{qs}/R_l \tag{16}$$

$$i_{ld} = v_{ds}/R_l \tag{17}$$

In addition, the qd-axis excitation capacitance currents are given by the following.

$$i_{cd} = i_d - i_{ld} \tag{18}$$

$$i_{cq} = i_q - i_{lq} \tag{19}$$

On the other hand, the qd-axis transient equivalent voltages can be expressed as shown below.

$$p\,V_{ds} = \omega_r\,V_{qs} + i_{cd}/C \tag{20}$$

$$p\,V_{qs} = \omega_r\,V_{ds} + i_{cq}/C \tag{21}$$

The electromagnetic torque can be expressed, in terms of qd-axis stator flux linkages and currents, as follows.

$$T_e = \frac{3}{2} P(\lambda_{ds} * i_{qs} - \lambda_{qs} * i_{ds}) \tag{22}$$

The mechanical equations can be written as given below.

$$T_m = T_e + J\,p\omega_r + B\omega_r \tag{23}$$

Finally, the machine power angle, δ, is given by the following.

$$\delta = \int (\omega_r - \omega_s) dt \tag{24}$$

4. Experimental setup

Figure 3 shows the experimental setup of a three-phase synchronous reluctance generator rated at 0.5 kW, 380 V, 50 Hz, and 4-pole. The experimental rotor, shown in Figure 4, is a salient-pole reluctance rotor made of laminated steel. The laminated rotor is obtained by modifying a squirrel-cage induction machine rotor by notching the slotted lamination or symmetrically removing some rotor teeth as shown in Figure 4. It is well known that the existence of the rotor cage improves both the starting and transient behavior. In other words, the rotor cage improves the stability characteristics of the generator due to its damping during any disturbance or oscillations in the wind speed [9]. The prime mover is a shunt DC-motor rated at 1.1 kW. A suitable balanced 3-phase Δ-connected variable capacitor bank is connected to the generator terminals. In addition, a balanced three-phase variable resistive load is used. The parameters of the machine were measured using standard techniques and are listed in Table 1. A dSPACE (DS1103) digital signal processor card was used for data acquisition purposes. Moreover, a voltage transducer (LV 25-P) as well as a DC tachogenerator were used to measure and detect both the generated voltage and the generator speed and hence were fed to the DSP through the signal conditioning circuit.

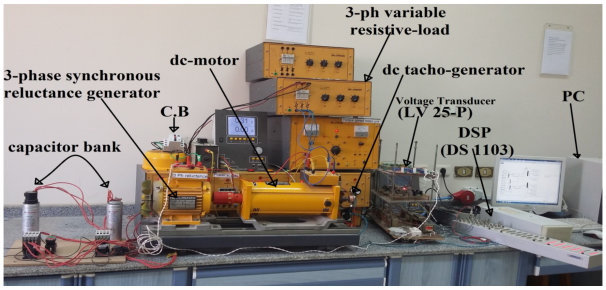

Figure 3. Experimental set-up.

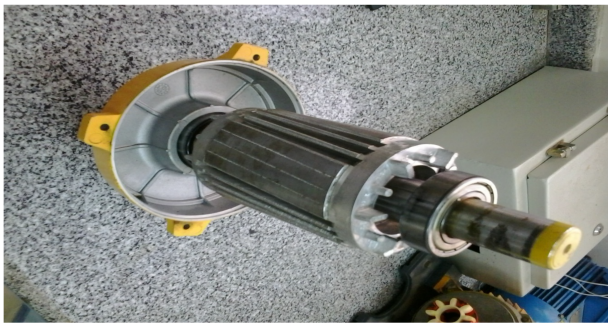

Figure 4. Photograph of the synchronous reluctance rotor.

Table 1. Parameters of synchronous reluctance generator.

Stator winding resistance, r_a	12 (Ω)
Stator leakage reactance, L_s	11.5 (Ω)
Rated current, I	2.1 (A)
q-axis stator reactance, X_{qs}	57 (Ω)
d-axis stator reactance, X_{ds}	166 (Ω)
q-axis rotor leakage reactance, X_{qr}	21.3 (Ω)
d-axis rotor leakage reactance, X_{dr}	17.4 (Ω)
q-axis rotor resistance, r_{qr}	17.3 (Ω)
d-axis rotor resistance, r_{dr}	17.1 (Ω)
q-axis magnetization reactance, X_{mq}	45.5 (Ω)
d-axis magnetization reactance, X_{md}	154 (Ω)
Viscous friction, B	0.000005 (Nm/rad/s)
Moment of inertia, J	0.0015 (kg m)

5. Simulation and experimental results

In order to confirm the validity of the proposed analysis for the self-excited wind-generating system, a series of experimental tests were performed on the three-phase synchronous reluctance generator.

The magnetization characteristics of the employed synchronous reluctance generator, which represent the relation between the d-axis magnetizing inductance and the corresponding magnetizing current, are shown in Figure 5.

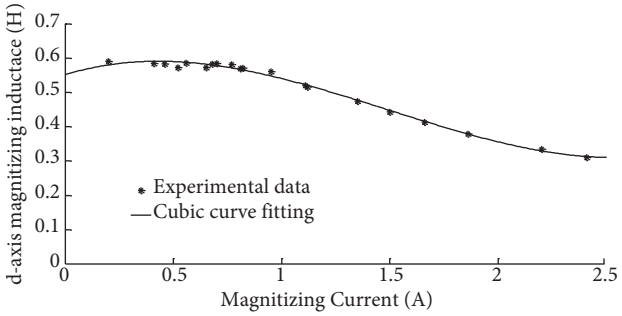

Figure 5. Magnetization characteristics of the employed SESRG.

Simulation results were obtained by solving the aforementioned models using MATLAB/Simulink software. The presented simulation results were obtained using the same parameters of the employed synchronous reluctance generator. However, the prime mover is a wind turbine. The parameters for the used wind turbine are listed in Table 2. In addition, in the simulation process, a third-order curve fitting is used to represent the magnetization characteristics as shown in Figure 5. The resulting cubic equation that relates the machine d-axis magnetizing inductance as a function of the d-axis stator current (magnetizing current) can be written as:

Table 2. Parameters of wind turbine.

Wind turbine power rating	1.25 (kW)
Air density, ??	1.225 (kg/m^3)
Rated wind speed	12 (m/s)
Wind energy utilizing ratio, Cp	0.315
Blade diameter, R	1.25 (m)
pitch angles, β	0–7 (degrees)

$$L_{md} = 0.0597 i_d^3 - 0.2664 i_d^2 + 0.1957 i_d + 0.5522. \quad (25)$$

In the following subsections, the effect of wind-speed variation, excitation-capacitors variation, and loading-conditions variation on the generated output voltage and frequency are presented and discussed.

5.1. Effect of wind-speed variation

Figure 6 shows the simulated results for the effect of wind-speed variation on the no-load generated voltage and frequency of the SESRG at a constant excitation capacitance of 41.1 μF. The wind speed varies from 9 m/s to 7 m/s through three different levels as shown in the figure. It can be observed that the generated voltage and frequency are sensitive to wind-speed variations. The reduction in wind-speed level results in decreasing both the generated voltage and frequency of the SESRG. Moreover, it can be noted that the frequency of the generated voltage is directly related to the prime-mover speed. This is due to the synchronization behavior of the employed machine.

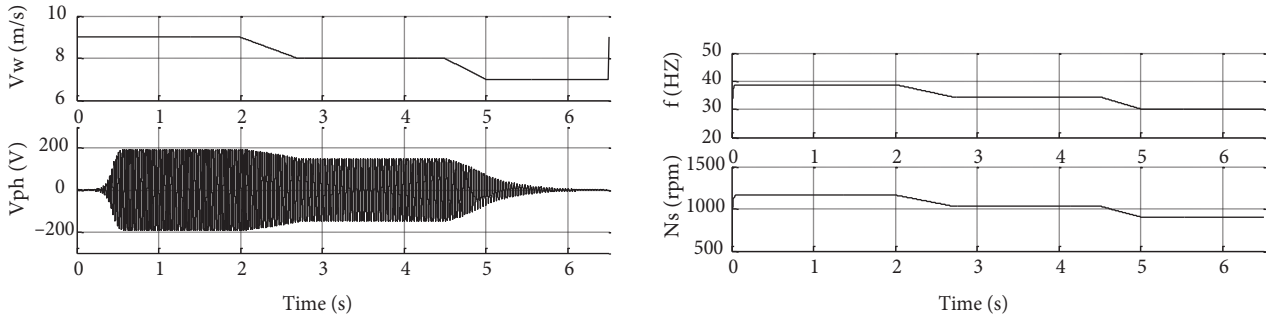

Figure 6. Effect of wind-speed variation on the no-load generated voltage and frequency at a constant excitation capacitance of 41.1 μF.

In addition, Figure 6 shows that, at a given excitation capacitance there is a critical minimum value of wind speed below which the generated voltage reaches zero. This critical value of the wind speed depends mainly upon the loading and excitation conditions. Therefore, the system can be operated in a wide range of wind speed if the excitation capacitance is changed with appropriate values according to the wind-speed variation.

Under the same excitation conditions, the measured generated phase-voltage of the SESRG at different values of prime-mover speed (DC-shunt motor) is shown in Figure 7.

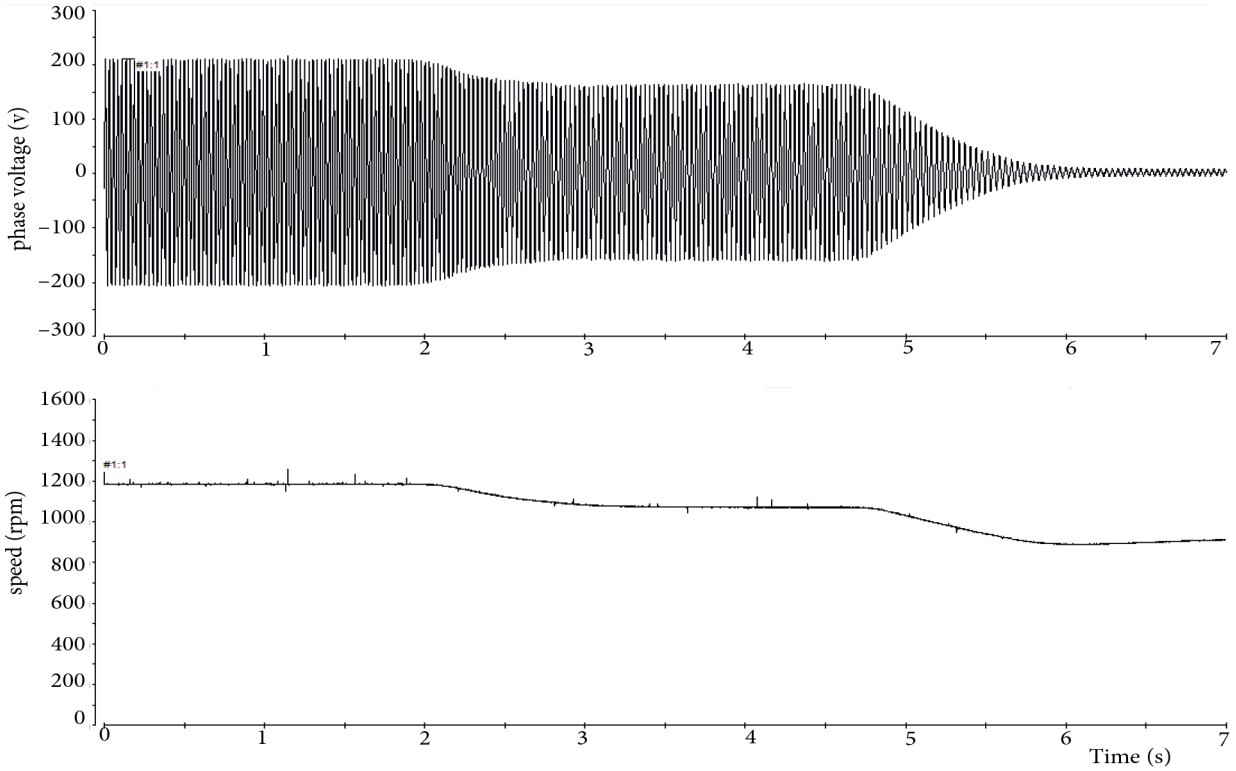

Figure 7. Variation of the measured no-load generated phase-voltage due to variation of the prime-mover speed at a constant excitation capacitance of 41.1 μF.

In the experimental process, a balanced three-phase, Δ-connected capacitor bank, each with 13.7 μF, is connected at the stator terminals of the synchronous reluctance generator. In addition, the speed of the DC-shunt motor is controlled to give the same behavior of the resultant system speed obtained in the simulation

process. A close correlation between both the simulated results and the corresponding measured results can be easily observed.

5.2. Effect of excitation-capacitance variation

At constant loading conditions and an appropriate value of wind speed, it is found that the generated voltage is very sensitive to any variation in the excitation-capacitance values. Figure 8 shows the simulated results for the effect of excitation-capacitance variation on the no-load generated voltage and frequency of the SESRG at a constant wind speed of 10 m/s. The presented results are obtained using three different values of excitation capacitance, 35 μF, 24.66 μF, and 20 μF, as shown in the figure.

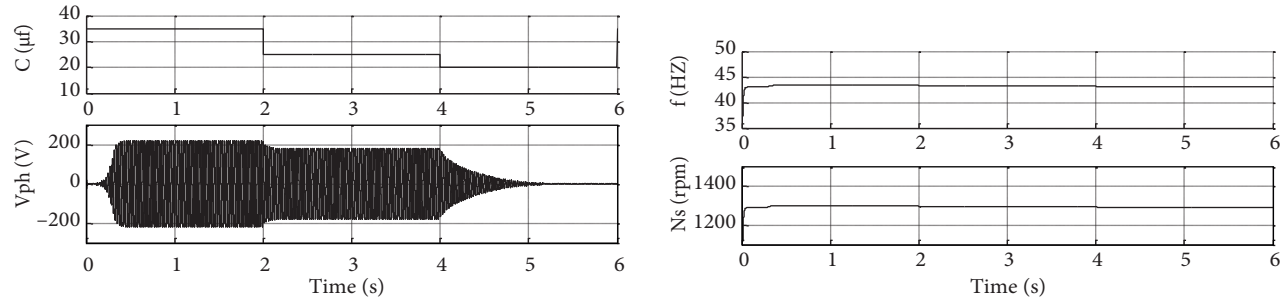

Figure 8. Effect of excitation-capacitance variation on no-load generated voltage and frequency at a constant wind speed of 10 m/s.

The obtained results ensure the sensitivity of the generated phase voltage to the excitation-capacitance variations. Figure 8 shows that reducing the value of the excitation capacitance results in decreasing the generated output voltage. Moreover, it is clear that there is a critical minimum value of the excitation capacitance below which the machine fails to generate voltage, as shown in Figure 8. In addition, it is found that the time taken by the SESRG during the build-up process is inversely proportional to the excitation-capacitance level.

The measured no-load phase-voltage of the SESRG at an excitation capacitance of 24.66 μF (balanced three-phase, Δ-connected capacitor bank, each with 8.22 μF) and constant prime-mover speed is shown in Figure 9.

5.3. Effect of loading-conditions variation

The effect of varying loading conditions on the generated voltage and frequency at constant wind speed and an appropriate value of excitation capacitance is shown in Figure 10. In the simulation process, the load resistance varies from no-load (simulated as a very high resistance) to 400 Ω at 1.5 s and to 150 Ω at 2.5 s. However, the excitation capacitance and wind speed are kept constant at 24.66 μF and 11 m/s, respectively.

It can be noted that when the load of the SESRG is increased (i.e. load resistance is decreased), the generator speed is decreased. This results in a great reduction in both the generated phase-voltage and frequency. In addition, there is a critical value of the load resistance below which the machine voltage collapses.

Under the same previous loading conditions, the variation of the measured generated phase-voltage due to the variation of the load resistance at a constant excitation-capacitance of 24.66 μF, without controlling the prime-mover speed, is shown in Figure 11.

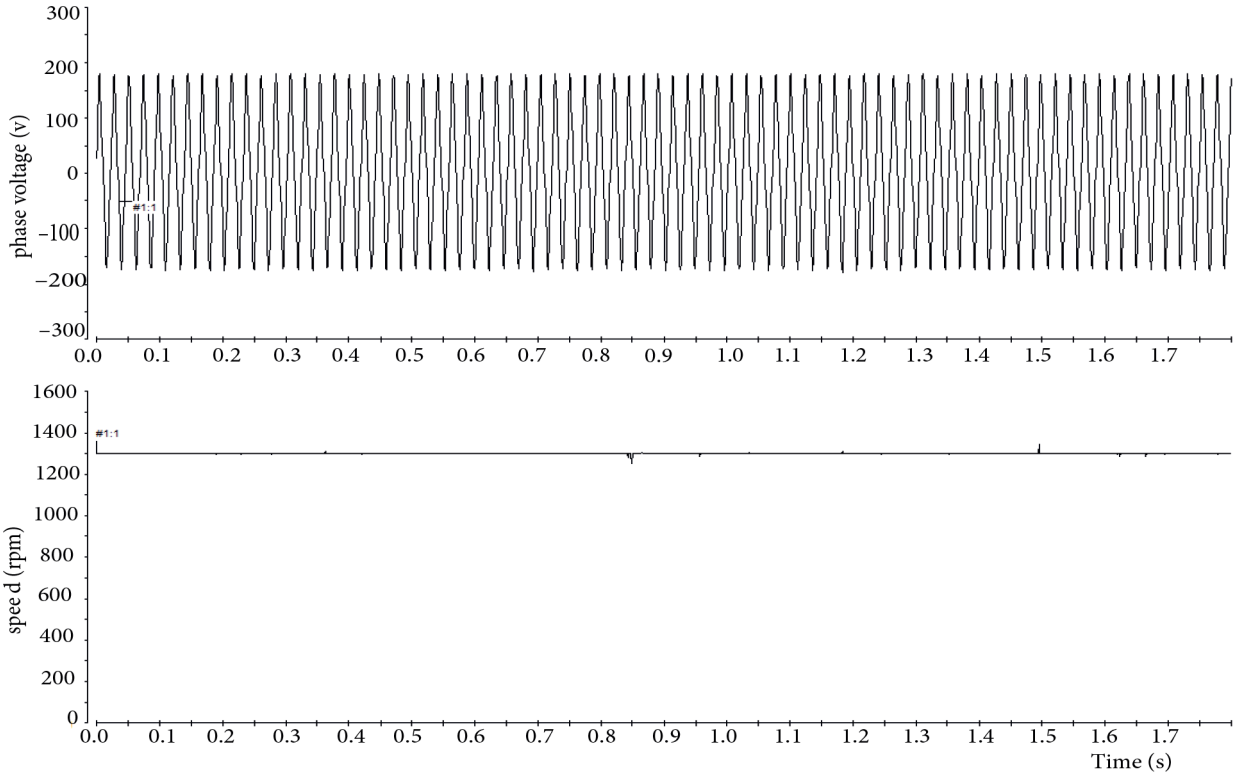

Figure 9. Measured no-load phase-voltage with at an excitation capacitance of 24.66 μF and constant prime-mover speed.

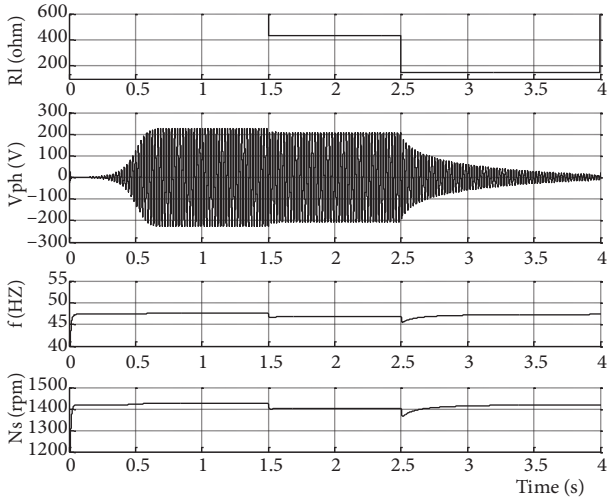

Figure 10. Variation of the generated voltage and frequency with different loading conditions at constant excitation capacitance of 24.66 μF and constant wind-speed of 11 m/s.

The discrepancy between the simulated and measured results, shown in Figures 10 and 11, is due to the different characteristics of the simulated wind turbine and the experimental DC-shunt motor when the generator is loaded.

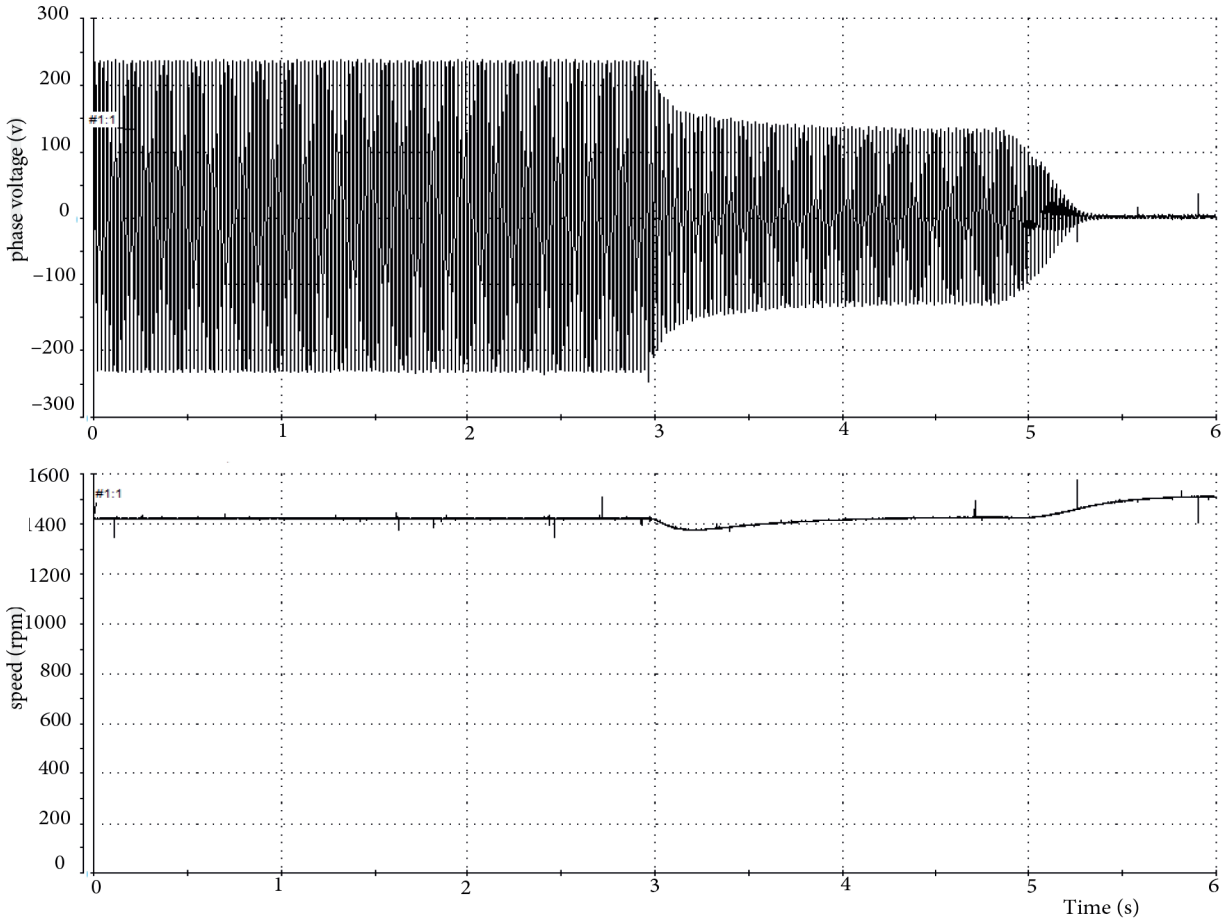

Figure 11. Variation of the measured generated phase-voltage due to variation of the load resistance at a constant excitation capacitance of 24.66 μF.

5.4. Conclusions and future works

This paper has presented a detailed analysis valid to predict the dynamic behavior of an isolated SESRG driven by a wind turbine. The build-up and self-excitation processes have been studied under different conditions. This paper has discussed the effect of wind-speed variation, excitation-capacitance variation, and loading-conditions variation on generated voltage and frequency. It has been observed that the frequency of the generated voltage is directly related to the prime-mover speed due to synchronization behavior of the employed generator. In addition, the presented results show that there is a critical minimum value of excitation capacitance below which the machine fails to generate voltage. It was found that the wind speed as well as the loading conditions directly affect the critical value of the excitation capacitance.

A close correlation between the experimental and simulated results was found, which verifies the validity of the proposed analysis. The paper conclusively proves that the proposed self-excited wind generating system may be a promising alternative to conventional synchronous generators. The proposed system may be used to feed loads that are insensitive to voltage or frequency deviations, such as heaters, water pumps, lighting, battery charging, etc.

Moreover, the obtained performance characteristics represent the basic tools required to develop a complete control system to regulate the generated voltage and frequency over a wide range of wind-speed variations.

Nomenclature

P_w	Power drawn by wind turbine (W)
ρ	Specific density of air (kg/m)
A	Area of the turbine blades (m^2)
V_w	Wind speed (m/s)
P_m	Mechanical power (W)
C_p	Rotor power coefficient
λ	Turbine tip-speed ratio
β	Blade pitch-angle (degrees)
R	Radius of the turbine blade (m)
ω_r	Rotor speed (rad/s)
T_m	Mechanical torque (Nm)
V_{ds}, V_{qs}	Stator voltages in d and q axes (V)
i_{ds}, i_{qs}	Stator currents in d and q axes (A)
λ_{ds}, λ_{qs}	Stator flux linkage in d and q axes (Wb)
λ_{dr}, λ_{qr}	Rotor flux linkage in d and q axes (Wb)
L_{md}, L_{md}	Magnetizing inductance in d and q axes (H)
L_{ds}, L_{qs}	Stator leakage inductance in d and q axes (H)
L_{dr}, L_{qr}	Rotor leakage inductance in d and q axes (H)
i_{cd}, i_{cq}	Capacitor current in d and q axes (A)
I_{ld}, i_{lq}	Load current in d and q axes (A)
r_a	Stator winding resistance (Ω)
r_{dr}, r_{qr}	d and q axis rotor resistance (Ω)
R_l	Load resistance (Ω)
P	Number of pole pairs
C	Excitation capacitance (F)
P	Differential operator (d/dt)
P_e	Electrical power (W)
T_e	Electromagnetic torque (Nm)
J	The overall system effective inertia (kgm^2)
B	Viscous friction coefficient (Nm/rad/s)
δ	Power angle (rad)
ω_s	Synchronous speed (rad/s)

References

[1] Wu B, Lang Y, Zargari N, Kouro S. Power Conversion and Control of Wind Energy Systems. Hoboken, NJ, USA: Wiley, 2011.

[2] Babu BC, Mohanty K. Doubly-fed induction generator for variable speed wind energy conversion systems-modeling & simulation. International Journal of Computer and Electrical Engineering 2010; 2: 141-148.

[3] Allam S, El-Khazendar M, Osheiba A. Steady-state analysis of a self-excited single-phase reluctance generator. IEE T Energy Conversion 2007; 22: 584-591.

[4] Wang YS, Wang L. Minimum loading resistance and its effects on performance of an isolated self-excited reluctance generator. IEE Proc-C 2001; 148: 251-256.

[5] Allam S, El-Khazendar M, Osheiba A. Dynamic analysis of a self-excited single-phase reluctance generator. Electr Pow Compo Sys 2006; 34: 725-738.

[6] Tokunaga S, Kesamaru K. FEM simulation of novel small wind turbine generation system with synchronous reluctance generator. In: IEEE 2011 Electrical Machines and Systems International Conference; 20–23 August 2011; Beijing, China. New York, NY, USA: IEEE. pp. 1-6.

[7] Seyoum D, Grantham C, Rahman MF. The dynamic characteristics of an isolated self-excited induction generator driven by a wind turbine. IEE T Ind Appl 2003; 39: 936-944.

[8] Joshi D, Sandhu KS, Soni MK. Voltage control of self-excited induction generator using genetic algorithm. Turk J Elec Eng & Comp Sci 2009; 17: 87-97.

[9] Rahim Y, Fletcher JE, Hassanain N. Performance analysis of salient-pole self-excited reluctance generators using a simplified model. IET Renew Power Gen 2010; 4: 253-260.

[10] Mohamadein A, Rahim Y, Al-Khalaf A. Steady-state performance of self-excited reluctance generators. IEE Proc-B 1990; 137: 293-298.

[11] Rana SD, Kar N. Steady-state analysis of self-excited synchronous reluctance generator. in: IEEE 2008 Electrical and Computer Engineering Conference; 4–7 May 2008; Niagara Falls, Canada. New York, NY, USA: IEEE. pp. 1617-1620.

[12] Alolah A. Capacitance requirements for three phase self-excited reluctance generators. IEE Proc-C 1991; 138: 193-198.

[13] Osheiba A, Rahman M. Performance analysis of self-excited induction and reluctance generators. Electr Mach Pow Syst 1991; 19: 477-499.

[14] Guha S, Kar NC. A linearized model of saturated self-excited synchronous reluctance generator. In: IEEE 2005 Electrical and Computer Engineering Conference; 1–4 May 2005; Canada. New York, NY, USA: IEEE. pp. 633-636.

[15] Rahim Y, Alyan M. Effect of excitation capacitors on transient performance of reluctance generators. IEE T Energy Conversion 1991; 6: 714-720.

[16] Rahim Y, Al-Sabbagh A. Controlled power transfer from wind driven reluctance generator. IEE T Energy Conversion 1997; 12: 275-281.

[17] Boldea I, Fu Z, Nasar S. High-performance reluctance generator. IEE Proc-B 1993; 140: 124-130.

[18] Abu-Elhaija WS, Muetze A. Self-excitation and stability at speed transients of self-excited single-phase reluctance generators. IEE T Sustain Energ 2013; 4: 136-144.

[19] Bharanikumar R, Kumar AN. Performance analysis of wind turbine-driven permanent magnet generator with matrix converter. Turk J Elec Eng & Comp Sci 2012; 20: 299-317.

[20] Hilmy M, Ahmed M, Orabi M, El-Nemr M. Modeling and control of direct drive variable speed stand-alone wind energy conversion systems. In: MEPCON'10 2010 International Middle East Power Systems Conference; 9–21 December 2010; Cairo, Egypt. pp. 19-21.

[21] Wang L, Wang YS. Dynamic performance and minimum loading effects of an isolated self-excited reluctance generator. In: IEEE 1999 Power Engineering Society Winter Meeting Conference; 31 January–4 February 1999. New York, NY, USA: IEEE. pp. 13-18.